7-21-2014

Contrasting Leaf Shapes Vary in Extent of Solar Tracking: Revisiting Darwin's "Service to the Plant"

Kerri Mocko
kerri.mocko@uconn.edu

Contrasting Leaf Shapes Vary in Extent of Solar Tracking:

Revisiting Darwin's "Service to the Plant"

Kerri Mocko

Contrasting Leaf Shapes Vary in Extent of Solar Tracking: Revisiting Darwin's "Service to the Plant"

Kerri Mocko

B.S., University of Connecticut, 2007

A Thesis

Submitted in Partial Fulfillment of the

Requirements for the Degree of

Master of Science

At the

University of Connecticut

2014

APPROVAL PAGE

Master of Science Thesis

Contrasting Leaf Shapes Vary in Extent of Solar Tracking:

Revisiting Darwin's "Service to the Plant"

Presented by

Kerri Mocko, B.S.

Major Advisor_____
Cynthia S. Jones

Associate Advisor_____
Robin L. Chazdon

Associate Advisor_____
John A. Silander, Jr.

Associate Advisor_____
Carl D. Schlichting

University of Connecticut
2014

Acknowledgements

I have been intrigued by South Africa since I set eyes on its landscape in 2007. While I'm totally captivated by its terrain, oceans and herds of animals, for me, one of the truly remarkable things is how dynamic of a place it is. Some of my favorite days are those that start with a heavy morning dew, the kind that you expect to linger for hours, that then dries up in an hour of sunlight and hums with buzzing pollinators throughout the afternoon. South Africa has taught me how quickly things change, and to open my eyes and observe in a way that I never had before. As I owe South Africa for the inspiration of a lifetime, I owe the people who have been there through my Master's degree and continue to be there as a forge ahead on my PhD.

I would like to thank the members of my committee, Robin Chazdon, John Silander and Carl Schlichting for their patience and flexibility with the completion of this project and for valuable comments on the manuscript. I would also like to thank Katie Dobbins and Matt Martin for encouraging me to complete this work and get my Master's degree. I especially thank Lauren Martin for her work on the shade analysis of the leaf images, and for being more than a sister could ask for in terms of the science and everything else non-science. Together, I thank Lauren, Matt, Katie and Nala for all the good times together and for reminding me to maintain a work-life balance.

I would also like to thank members of the Jones lab, past and present. Jessica Budke, Caroline Chong, Hugo Martinez and Dustin Ray have been there for me

through all phases of the science, from brainstorming ideas, to collecting data, to completing projects. I am especially thankful for their companionship in the lab and field.

I would like to thank Cindi most of all. Cindi has been my most important mentor, exposing me to plant structure and function, sharing her expertise and excitement for science, and further instilling my passion for all things botanical. Personally, I am grateful for her friendship and sticking with me through the tough times.

Lastly, I would like to thank my parents for teaching me to go after my goals and for their endless support, patience and belief in me.

This project would not be possible without funding from the National Science Foundation, NSF-IRE (OISE-0623341) and NSF-Dimensions of Biodiversity (1046328). I would also like to thank Cape Nature for collection permits and De Hoop Nature Reserve for permission to collect.

Table of Contents

Summary……1

Introduction……3

Materials and methods……7

Results……16

Discussion……24

Conclusion……30

References……31

Tables and Figures……37

Appendix……51

Summary

1. Solar tracking affects leaf temperature through the amount of direct light intercepting the lamina. However, leaf shape also affects leaf temperature due to heat transfer across boundary layers, and no studies have addressed the effect of leaf shape on solar tracking and leaf temperatures in the field.
2. We compare solar tracking, leaf temperatures, photosynthetic rates and leaf longevity in two co-occurring species with contrasting leaf morphologies: *Pelargonium lobatum* has a large, shallowly lobed leaf and *P. triste* has a highly dissected leaf composed of many small leaflets.
3. *Pelargonium triste* tracked the sun more closely than *P. lobatum*, although *P. lobatum* intercepted more direct light at midday despite less solar tracking. Leaf temperatures for the two species were more similar than predicted based on leaf energy budgets. Photosynthetic rates declined more in *P. lobatum* than *P. triste* at the end of the growing season and *P. triste* leaves were estimated to live 20% longer.
4. Leaf three-dimensionality has thermal effects beyond that predicted from a traditional energy budget equation. By moving, *P. triste* leaves heat up quickly in the morning yet experience little direct light at midday from self-shading leaflets. *Pelargonium lobatum* leaves warm more slowly but reach the same maximum temperature as *P. triste*. We hypothesize that the one-month longer life span of *P. triste* leaves is in part due to the avoidance of lethal leaf temperatures as summer approaches.

5. The combination of leaf shape and solar tracking may be directly linked to differences in leaf longevity in these exposed geophytes through their modulation of direct light absorption and the downstream effects on leaf thermodynamics and photosynthetic rate. Leaf shape may predict leaf function better than many commonly measured functional traits, and the full extent of Darwin's "service to the plant" results from the synergistic effects of leaf movement and morphology.

Introduction

Solar tracking in plants describes the temporary and reversible movement of leaves in response to light. Darwin (1881) recognized that this phenomenon provided a "service to the plant" that has since been studied by ecophysiologists, most extensively in arid environments (Ehleringer & Forseth 1980). Under cool temperatures and non-water stressed conditions, many plants tend to display diaheliotropic movements that maintain leaves perpendicular to incident light, maximizing photon flux density to achieve high photosynthetic rates throughout the day. Under hot, dry conditions, paraheliotropic movements parallel to solar incidence reduce photon flux density to prevent thermal damage and enhance water use efficiency.

Examined mostly in species with pinnately compound leaves and pulvini at the base of leaflets, there has been little direct attention to the effect of leaf shape on the extent of solar tracking. Leaf energy exchange with the environment depends on the physical properties of a given leaf shape such that an entire leaf has a thicker boundary layer and less heat transfer with the environment than a highly dissected leaf (Schuepp 1993). Therefore, dissected leaves are predicted to maintain temperatures closer to ambient. However, energy budgets for any shape of leaf can be influenced by changes in leaf angle.

Much of what is known about the effects of leaf shape and boundary layers on leaf temperature have been addressed primarily in a theoretical context, e.g. separate experiments in wind tunnels and on flat-plate objects of different shapes

(Pearman, Weaver & Tanner 1972; Grace, Fasehun & Dixon 1980). The relatively few studies that have been done in the field suggest that leaf temperatures rarely are as different from ambient as predicted from leaf energy budget calculations, even across a range of leaf types (Gates, Alderfer & Taylor 1968; Geller & Smith 1982) because in the field, temperatures are also affected by windspeed, transpirational cooling and shading by neighbors. Few studies have compared temperatures between leaves that contrast in shape and size in the same sites at the same time (but see Hegazy and El Amry (1998)). Consequently, we still lack a comprehensive picture of the "service to the plant" provided by leaf movements in leaves that differ in shape.

A unique opportunity to examine the influence of leaf shape on solar tracking among co-occurring species is presented in the Cape Floristic Region (CFR) of southern Africa. The CFR has a Mediterranean climate characterized by hot, dry summers and cool, wet winters as well as relatively high diversity of geophytic species (Rossa & von Willert 1999; Goldblatt & Manning 2002), many of which show some degree of solar tracking (Esler, Rundel & Vorster 1999). Because winter is the primary growing season for most ephemeral and seasonally apparent species and many geophytes are summer-deciduous, we expect that species capable of solar tracking will exhibit diaheliotropic movements during the winter to maximize light energy and optimize temperatures for photosynthesis.

To examine the interactions among leaf shape, solar tracking, light absorption and leaf temperatures in the field, we chose two species of *Pelargonium* endemic to South Africa. These sister species share a common geophytic growth

form and co-occur at some sites. However, they exhibit striking differences in leaf shape variation: *P. triste* has pinnately-veined leaves dissected to the midrib and composed of small (1 mm wide) leaflets, while *P. lobatum* has shallowly lobed and palmately-veined leaves (Fig. 1). Their geophytic growth form has the advantage that interpretations of leaf movements are not complicated by species differences in plant architecture: both species have leaves grow in rosettes from below-ground tubers. *Pelargonium* species do not have pulvini, and thus fall into the group of solar-tracking species that achieve leaf movements through petiole twisting (Galvez & Pearcy 2003) or changes in turgidity in cells across the leaf (van Zanten *et al.* 2010).

Our first goal was to determine whether *P. triste* and *P. lobatum* exhibit differences in movement, and if these movements are consistent with solar tracking by increasing photosynthetic carbon gain and/or fitness (Mooney & Ehleringer 1978; Forseth & Ehleringer 1983). If species exhibit solar tracking, our second goal was to determine whether leaf movements influence leaf temperature and light interception. We were also interested in knowing whether temperatures measured in the field are consistent with predictions from boundary layer theory based on leaf shape. The extent to which solar tracking effectively facilitates a favorable leaf energy balance depends in large part on the physical dimensions of the leaf. The thickness of the boundary layer, the insulating layer of dead air space over the surface of the leaf, depends on the width of the leaf in the direction of air flow (Nobel 1983; Schuepp 1993). A large leaf has a thicker boundary layer than a small leaf, and under similar conditions, leaf energy budget equations predict that the

large leaf will heat up more quickly and will end up with higher temperatures. In small leaves or leaflets, thin boundary layers enhance convective heat exchange with the environment so leaf temperatures will be closer to ambient. Because leaf shape determines functional leaf size, a leaf composed of lobes or leaflets will have a thinner and more broken boundary layer than an entire leaf (Schuepp 1993), all else being equal.

Therefore, we had two competing hypotheses. One hypothesis is that larger leaves heat up more quickly and reach much higher leaf temperatures, regardless of mitigating effects of solar tracking. In other words, leaf morphology would dominate any effect of moving. Our alternative hypothesis was that solar tracking has greater effect on leaf temperatures than leaf shape. If light interception is the primary driver of leaf temperatures, then leaves that track the sun more closely heat up more quickly and have higher leaf temperatures, thus solar tracking will override the thermal effects of leaf morphology. Finally, we seek to examine the full "service to the plant" by scaling up to daily and seasonal carbon gain.

Materials and methods

Field measurements

We quantified solar tracking movements of *P. triste* and *P. lobatum* leaves across a diurnal time course at De Hoop Nature Reserve, a region characterized by fynbos vegetation (Cowling, Richardson & Pierce 1997) on the southern coast of South Africa (S 34°26'39.1" E 20°25'16.9"). *Pelargonium triste* and *P. lobatum* co-occur at De Hoop and are often found growing within one meter of each other in sandy soils with sparse vegetation. We tracked five leaves of each species (one leaf per plant) and made measurements every two hours from 07:00 to 17:00 on July 22, 2008. Leaf angle was measured as the angle of inclination of the lamina from horizontal using a protractor and a straight edge. For leaf azimuth, we used a compass to find the direction that the majority of the adaxial leaf surface was facing at the time of measurement. We measured adaxial leaf temperatures using an Optris® LaserSight (Optris GmbH, Berlin, Germany) infrared thermometer with a laser spotsize of 1 mm. Four or five point measurements were taken across each leaf surface at each time period to obtain a mean leaf temperature. Ambient air temperature and windspeed were obtained from a portable hand-held weather station (Kestrel 3500; KestrelMeters, Birmingham, MI, USA) and soil temperature around each leaf was found using the laser thermometer. We measured stomatal conductances of the abaxial and adaxial leaf surfaces with a steady state diffusion porometer, Decagon® Leaf Porometer Model SC-1 (Decagon, Pullman, WA, USA

purchased in 2007). Leaves were photographed (face-on view) at each observation to determine shading over the lamina.

All measured leaves were collected at the end of the day and kept hydrated for measurements of fresh weight and area. For determination of lamina dimensions and specific leaf area (SLA), we measured the flattened lamina area (cm^2) of the fresh leaves with a Li-Cor® 3100 leaf area meter (Li-Cor, Lincoln, NE, USA) as well as the overall lamina dimensions (length and width, cm). We dried laminae to obtain dry masses, and calculated SLA (cm^2/g) as the ratio of fresh leaf area to dry leaf mass. Functional leaf size (FLS) was determined as the diameter of the largest circle that could be inscribed within the dissected outline of the lamina (Jones *et al.* 2009).

We quantified leaf shape with a continuous leaf dissection index (LDI). LDI is the ratio of the perimeter of a leaf divided by the square root of the flattened leaf area. Values for LDI increase with leaf dissection. McClellan and Endler (1998) found that fractal dimension, which accounted for leaf three-dimensionality beyond perimeter and area measurements used to calculate LDI, was highly correlated with dissection index and revealed little additional information about shape. We used LDI and the difference between flattened leaf area measured with a Li-Cor® leaf area meter (Li-Cor, Lincoln, NE, USA) from collected leaves and projected area measured from the field photographs taken in face-view to quantify the extent of three-dimensionality in our system.

Leaf light interception calculations

Leaf energy input is determined primarily through direct light intercepting the leaf surface (Forseth & Teramura 1986). Cosine of interception (Cosine i) represents the proportion of the sun's direct beam that a leaf can potentially capture. Cosine i is a calculation based on the position of the leaf relative to the sun and is determined from leaf and sun angles as follows:

$$\cos i = \cos \beta \times \sin E + \sin \beta \times \cos E \times \cos (\alpha_s \times \alpha_l)$$

where β = leaf angle from horizontal

E = solar elevation

α_s = solar azimuth angle

α_l = leaf azimuth angle

Cosine i values range from -1 to1 with negative or positive values indicating illumination on the abaxial or adaxial leaf surface, respectively. A cosine i value of one represents the condition when the leaf blade is oriented perpendicularly to the sun's direct beam (i.e. orientation for maximum direct light interception). Cosine i values approach zero when the leaf blade is parallel to the sun's radiation and there is little potential for direct light capture (Prichard & Forseth 1988; Rosa & Forseth 1996). Solar data were obtained from the NOAA Earth System Research Lab Solar Position Calculator (Cornwall, Horiuchi & Lehman 2014).

Determining leaf shape parameter (K_l) from leaf boundary layer thickness (δ_{bl})

To determine leaf energy balance, we calculated leaf boundary layer resistance which then allowed us to calculate leaf boundary layer thickness. We determined leaf boundary layer resistances using the single leaf model described by Balding and Cunningham (1976). This model is used for determining the boundary layer resistance of small simple leaves, appropriate for our study system because we used functional leaf size (FLS) in the boundary layer resistance calculations (Parkhurst & Loucks 1972; Jones *et al.* 2013), assuming that aggregates of leaflets were not functioning as a whole leaf.

Boundary layer resistance (R''_a (s cm^{-1})) was calculated based on Balding and Cunningham (1976) as follows:

$$R''_a = K_a * \frac{D^x W^y}{V^z}$$

where K_a is a constant term depending on leaf size (see Table 1 in Balding and Cunningham (1976)), D and W are functional leaf length and width (perpendicular measurements of the long axis and short axis of the leaf, i.e. functional leaf size), V is the wind velocity and x, y and z are power terms that also depend on leaf size..

We then calculated boundary layer thickness (δ_{bl}) as the product of boundary layer resistance (R''_a) and the diffusion coefficient for water vapor (D_j) (Sousa 2003):

$$\delta_{bl} = R''_a \times D_j$$

We could then estimate the leaf shape parameter (K_l (mm $s^{-1/2}$)) for *P. triste* and *P. lobatum* using the following formula (Nobel 1983; Sousa 2003):

$$K_l = \delta_{bl} * (w/v)^{-1/2}$$

where δ_{bl} is the boundary layer thickness (mm), w is the leaf length in the direction of the wind (m) and v is the wind velocity (m s^{-1}). We performed these calculations for each individual *P. triste* and *P. lobatum* leaf that we followed across the diurnal time course.

Leaf energy balance calculations

Predicted leaf temperatures were obtained using an energy budget equation (Sousa 2003), see Appendix Table 1 for equation and definition of terms. To calculate actual leaf temperatures for each time observation, we input the proportion of the sun's direct beam intercepted by the leaf (cosine i), leaf length and width, the leaf shape parameter for each species (K_l), air temperature, windspeed and stomatal conductance. We used the energy budget equation to predicted leaf temperatures for *P. triste* and *P. lobatum* leaves throughout the day based on their observed movements, and compared these predictions to actual measured leaf temperatures in the field. To examine the specific effect of solar tracking, we also calculated expected leaf temperatures for leaves that did not move during the day (i.e. zero leaf inclination, to simulate leaves positioned flat on the ground). Energy budgets were calculated separately for individual leaves at each time.

Image analysis of leaf shape and light regime

We used Adobe Photoshop CS4 Extended (2008) to analyze the light regime over the leaf surfaces of *P. triste* and *P. lobatum* on face-view photographs of the leaves at each measurement period across the diurnal time course. Light on the leaf surface was categorized as direct, diffuse or shade using the Threshold command and Color Matching for individual pixels across the laminas. We used the Magic Wand Selection Tool to then select and calculate the total areas of direct light, diffuse light and shade (Adobe Photoshop CS4 Extended 2008) (Fig. 2). We also used Photoshop to determine the total projected leaf areas.

Photosynthetic rates

Photosynthetic rates of *P. triste* and *P. lobatum* populations at De Hoop were measured in 2012 as a part of a larger survey of photosynthetic rates of *Pelargonium* species in the field in South Africa. Maximum rates of photosynthesis were measured at three time points during the growing season (July 26, August 27 and October 6) to examine variation in photosynthetic rates mid-to-late season. At each time, maximum rates of photosynthesis were measured on 4-8 individuals per population, and the same plants were used for photosynthetic measurements throughout the course of the season. We measured photosynthetic rates on the most recently, fully expanded leaf on each plant; we measured one leaf per plant and calculated species means for each time point.

Gas exchange measurements were made between 9:00 and 11:00 AM. We measured light-saturated rates of photosynthesis per unit leaf area using a Li-Cor 6400XT with a CO_2 mixing system and a red/blue LED light source (Li-Cor, Lincoln, NE, USA). CO_2 concentration was maintained at 400 μmol mol^{-1}; flow rate at 500 μmol s^{-1}; PAR inside the chamber at 1500 μmol m^{-2} s^{-1} and chamber humidity was maintained slightly below ambient. We made three gas exchange measurements per leaf: the first measurement was made after one minute and then the next two measurements every 30 seconds after. We took the average of these three readings to determine the mean photosynthetic rate per leaf. The chamber was closed and empty for at least a minute in between measurements, and we regularly matched sample and reference cells to correct for drift in the CO_2 and H_2O sample cell values.

Leaf Longevity

To quantify leaf longevity, we tagged and monitored leaf development on each of 12 individual plants of each species at De Hoop throughout the main growing season in 2012 (July to October). Seven censuses were conducted over the 109 day monitoring period. At each census, leaf initiation, growth and senescence were recorded. In total, we tracked leaf survival across 72 individual leaves in *P. lobatum* and 62 leaves in *P. triste*. To estimate age-specific survival probability distributions for each species we used Bayesian survival trajectory analysis (BaSTA 1.9.3, (Colchero, Jones & Rebke 2012). Leaf survivorship was compared across the

census period and species leaf longevity expressed as leaf life expectancy (number of days) estimated at 100 days post leaf initiation.

Leaf anatomy

Leaves were fixed in FAA, dehydrated through a graded alcohol series and embedded using a JB-4 embedding kit (PolySciences, Inc., Warrington, PA., USA). Leaf sections were cut 5 μm thick, stained with toluidine blue and viewed under a light microscope.

Statistical analyses

Data were analyzed using R version 2.15.2 (R Development Core Team 2012). *Pelargonium triste* and *P. lobatum* measurements across the diurnal time course were analyzed using two different approaches: we used ANOVA in the base R package and a Generalized Least Squares (gls) Repeated Measures Analysis using the gls() function in the *nlme* library. For the gls, we examined four possible models for the correlation structure of the repeated measurements: compound symmetry, completely unstructured with possibly unequal variances, AR(1) with equal variances, AR(1) with unequal variances. We performed a likelihood ratio test to compare these models to determine how to structure the analysis, and used the gls model to identify parameters that significantly affected leaf temperatures. We also used ANOVAs to compare mean differences in leaf traits, leaf temperatures, the

extent of movement, potential light interception and actual light regime on the leaf surfaces. Photosynthetic rates were analyzed with an ANOVA and Tukey HSD to test for difference between species and seasons.

Results

Leaf morphology

Despite differing in the degree of dissection, overall lamina lengths and widths for each species were not significantly different (Table 1). The higher LDI of *P. triste* resulted in significantly lower leaf areas. *P. triste* also had a lower mean SLA than *P. lobatum.* These differences in structure were associated with differences in rates of stomatal conductance, which were slightly but not significantly higher in *P. triste*. Both *P. triste* and *P. lobatum* exhibited some three-dimensional structure (see leaves in profile-view, Figs 3a and 8) that we quantified as the difference between flattened and projected leaf area (D). This difference was ~4.5 cm^2 for both species, although this was a significantly larger proportion of the total leaf area for *P. triste* (29%) than *P. lobatum* (10%).

Leaf movements and leaf temperatures measured in the field

Leaves of both *P. triste* and *P. lobatum* were flat on the ground in the early morning (7:00) and inclined and rotated during the day. The leaf angles of both species changed significantly from zero throughout the day ($F=5.05$, $P=0.003$). Species differed in the overall extent of inclination: *P. triste* inclined more than *P. lobatum* ($F=9.09$, $P=0.017$) (Fig. 3a). Both species exhibited maximum leaf angles at midday (13:00) although *P. triste* leaves inclined to a mean maximum leaf angle of 47° compared to 24° in *P. lobatum*. The diurnal pattern of change in leaf angle was

similar for the two species, i.e. there was no species x time interaction (F=0.25, P=0.909). There were also significant changes in azimuth in leaves of both species across hours of the day (F=4.43, P=0.006) but there were no differences between species in the mean amount of azimuthal change (F=1.53, P=0.252), i.e. both species exhibited rotation, and similar amounts of rotation, during the day.

Cosine leaf angle is a useful metric for quantifying total leaf movement because it incorporates both changes in inclination and azimuthal rotation, i.e. cosine leaf angle is the product of the angle of inclination and the change in azimuth. Early in the morning, both species had cosine leaf angles of one, which indicates no movement (no inclination, no rotation). Cosine leaf angle in *P. triste* dropped to 0.3 at midday and only to 0.8 in *P. lobatum*, illustrating greater total movement in *P. triste* than *P. lobatum* across the diurnal time course (F=6.45, P=0.014) (Fig. 3b). Differences in cosine leaf angle were driven by differences in leaf angle between *P. triste* and *P. lobatum* because azimuthal change was similar across species.

These leaf movements ultimately resulted in differences in the degree of diurnal solar tracking between *P. triste* and *P. lobatum*: *P. triste* oriented to intercept more of the sun's direct beam than *P. lobatum* over the course of the day (F=7.33, P=0.027). Maximum orientation to incident light occurred in *P. triste* leaves at 11:00, which were oriented to potentially intercept 86% of the sun's direct beam (average maximum cosine i: 0.86). Maximum orientation to incident light in *P. lobatum* occurred at 13:00 when leaves were positioned to potentially intercept 54% incident light (cosine i=0.54). The amount of light interception changed similarly

throughout the day in both species; there were significant differences in cosine i (F=8.73, P=6.97e-05) but no significant species x time interaction (F=0.39, P=0.815).

Despite differences in the degree of solar tracking between species, leaf temperatures for *P. triste* and *P. lobatum* (F=0.686, P=0.43) did not differ from each other or from ambient (F=0.73, P=0.497) (Fig. 5); soil temperatures closely tracked ambient throughout the day. Leaf temperatures changed with ambient during the day in both species and the pattern of diurnal change in leaf temperature was similar for *P. triste* and *P. lobatum* (F=1.56, P=0.208).

Leaf temperatures of both species ranged from 12°C to 21°C but exhibited subtly different patterns of heating and cooling across the diurnal time course. By 9:00, leaves of *P. triste* had heated up more than leaves of *P. lobatum* and this was the only time during the day when there was a significant difference in leaf temperatures between the two species (Fig. 5, TukeyHSD P=0.05 for *P. triste* and *P. lobatum*). *Pelargonium triste* leaves reached their maximum temperature at 11:00; leaf temperatures stabilize throughout the middle of the day and cool gradually throughout the afternoon. In comparison, *P. lobatum* leaves take longer to heat up during the day and reach their maximum temperature at 13:00, then cool more rapidly at the end of the day; the only difference between ambient and any leaf temperatures at any time across the diurnal time course was at 17:00 when leaves of *P. lobatum* were significantly cooler than ambient (Fig. 5, TukeyHSD P=0.01 for *P. lobatum* and ambient).

Diurnal leaf temperature predictions and the effects of incident light and leaf shape

By 9:00, *P. triste* leaves were 2°C higher than ambient, due to their inclination angle of 31°(Fig. 6). Measured temperatures in the field were more than a degree warmer than expected for modeled stationary leaves that did not move and were also warmer than predicted from energy budget equations for leaves with this inclination, suggesting that early morning solar heating was greater than predicted based on cosine i alone (for numbers, see Appendix Table 2).

Examination of the pattern of direct and diffuse light across the surface showed that in *P. triste*, direct light interception is maximized in the early morning relative to any other time of the day (Fig. 7 and Appendix Fig. 1). On average, 51% of the lamina surface is exposed to direct sunlight. *P. triste* leaves are still lying relatively flat on the ground, and were these leaves flat surfaces, there would be little potential to intercept direct light. However, these leaves are strongly three-dimensional, and the upward projecting leaflets absorb considerable amounts of direct light (Fig. 8) with their nearly normal orientation to the sun, which is very low on the horizon in the early mornings of mid-winter.

By 11:00, *P. triste* leaves had inclined to an average angle of 42° and a 16° mean change in azimuth from the 9:00 direction. Measured leaf temperatures were again 2°C warmer than ambient on average and similar to temperatures predicted with leaf movement based on leaf energy budgets. Temperatures predicted from modeling these leaves without any leaf movement were slightly cooler. At this time,

50% of the leaf surface was intercepting direct light while the remaining surface experienced equal amounts of diffuse light and shade (Fig. 7).

By midday, *P. triste* leaves were a little more than a degree cooler than ambient and 2-3°C cooler than modeled temperatures for flat and inclined leaves due to increased shading and reduced direct light interception on the lamina (Figs 6 and 7, 13:00). At this time, 55% of the leaf area is shaded and only 25% of the lamina surface is in direct light. The highly-dissected leaf shape with leaflets projecting at odd angles to the plane of leaf angle measurement are responsible for the large proportion of shaded area when the sun is at its zenith. Although *P. triste* leaves are tracking the sun most closely at this time (i.e. the rachis is facing the sun), only the tips of the leaflets are exposed to direct light (Fig. 8).

At mid afternoon, observed leaf temperatures of *P. triste* were one degree warmer than ambient and slightly warmer than modeled predictions for inclined and flattened leaves. Direct light interception had increased at this time to 36% (from 25% at 13:00). At 15:00 the proportion of direct light increased relative to a few hours earlier because at low solar angles, and low leaf (rachis) angles, sunlight strikes more surface area on individual leaflets.

Late in the afternoon (17:00), leaf temperatures matched predictions for flat leaves despite an inclination of 37° and were about one degree cooler than ambient than was predicted for this observed inclination. There was no direct light on the leaf surface. The low solar angle of late afternoon resulted in considerable shading from other vegetation that did not permit the penetrance of any direct light.

P. lobatum leaves inclined to a lesser extent than *P. triste* leaves such that cosine i did not significantly increase from a stationary leaf at any time, nor did this limited movement result in the higher leaf temperatures predicted by energy budget calculations. That is, there was no difference in the predicted leaf temperatures for *P. lobatum* whether leaves were inclined at the observed angles or flat and stationary leaves (Fig. 6; for numbers, see Appendix Table 2). Actual leaf temperatures closely tracked ambient and were 4-7°C cooler than energy budget predictions throughout the day.

Leaves were cooler than ambient in the morning and heated slowly. At 9:00, only 30% of the leaf blade received direct light while 42%, was in complete shade. We attribute cooler leaf temperatures to self-shading over the leaf surface (Appendix Fig 1). While *P. lobatum* leaves are more like flat, two-dimensional plates than *P. triste* leaves, they all have some degree of cupping or curling at the margins that contributed some three-dimensionality. Self-shading, the low angle of the sun in the morning, and little solar tracking at this time resulted in leaves over 3 degrees cooler than *P. triste* leaves at the same time (Fig. 8).

By 11:00, leaf temperatures of *P. lobatum* had warmed to match ambient. The higher sun at 11:00 resulted in nearly 60% of the leaf in direct light (about twice as much as 9:00), with the remaining leaf area receiving equal amounts of diffuse light and shade. Observed leaf temperatures were still much cooler than expected from energy budgets. By midday (13:00), leaf temperatures had warmed to slightly above ambient yet observed mean leaf temperature was still nearly 7°C cooler than predicted based on energy budgets. The light regime on the surface of

the lamina was similar to that in late morning. At mid-afternoon, observed leaf temperatures were close to ambient, although still cooler than predicted, as a large proportion (~50%) of the lamina was now shaded and only 25% of the surface received direct light. By late in the afternoon, *P. lobatum* leaves were almost completely shaded; leaf temperatures at this time were slightly cooler than ambient.

Leaf anatomy and photosynthetic rates

Pelargonium triste and *P. lobatum* leaves differed dramatically in transectional symmetry and in distribution of photosynthetic tissues (Fig. 9). *Pelargonium triste* leaves had an isolateral distribution of palisade parenchyma cells while *P. lobatum* leaves are bilateral with palisade parenchyma on the adaxial side.

Despite differences in anatomy, area-adjusted photosynthetic rates were not significantly different between species at any time during the season (mid-July (P=0.54), late August (P=0.68) and early October (P=0.29)) although in October photosynthetic rates had declined more for *P. lobatum* (P=0.01) than for *P. triste* (P=0.34) as compared to earlier in the season (Fig. 10). Although the differences between species were not statistically significant, *P. lobatum* had photosynthetic rates that were slightly higher than *P. triste* in July and August and slightly lower than *P. triste* in October. Photosynthetic rates in *P. lobatum* were around 20 μmol CO_2 $m^{-2}s^{-1}$ in July and August (Tukey HSD P=0.98) and declined significantly to 13 μmol CO_2 $m^{-2}s^{-1}$ in October (Tukey HSD P=0.002). In *P. triste*, photosynthetic rates were around 18-19 μmol CO_2 $m^{-2}s^{-1}$ in July and August (Tukey HSD P=0.98) and 15

μmol CO_2 $m^{-2}s^{-1}$ in October, which was not a statistically significant decline from earlier in the season ((Tukey HSD P=0.14).

Leaf longevity

Pelargonium lobatum and *P. triste* have different survivorship curves and estimates of population-level leaf lifespan based on Bayesian survival trajectory analysis. Leaf lifespan is ~127 days for *P. lobatum* and ~153 days for *P. triste* (Fig. 11). *Pelargonium lobatum* and *P. triste* also have moderately different survival trajectories (survival probability versus leaf age): at a leaf age of 100 days, a single *P. triste* leaf has about a 50% chance of still being alive, while there is a 40% chance that a *P. lobatum* leaf will still be alive at 100 days. Beyond 100 days of age, differences in the probability of survival for a single leaf of each species are accentuated further such that the chance that a given leaf will be alive declines more rapidly for *P. lobatum* than for *P. triste*.

Discussion

Leaves of different shapes move differently. Highly dissected, pinnate *P. triste* leaves exhibit nearly twice as much inclination of the midrib as large, lobed *P. lobatum* leaves. Since leaves of *Pelargonium* species don't have pulvini, this movement is likely due to changes in turgor within the petiole and rachis that lead to declines in cell size on the adaxial surface and cause the leaf to curl, and these changes in curvature can occur in minutes (Fujita, Takagi & Terashima 2008; Fukuda *et al.* 2008). Similarly, curvature of the lamina is likely controlled by elongation of cells in the abaxial epidermis upon illumination on the adaxial leaf surface (Fukuda *et al.* 2008). Leaf angles also depend on mechanical and anatomical properties of the petiole (Niinemets 1998; Hernandez 2010). Venation architecture, leaf dimensions and shape, e.g. length-width ratio, may also constrain leaf movements (Hernandez 2010). For instance, leaf inclination in *P. lobatum* may be limited purely by the physical attributes of its leaves: the total mass of *P. lobatum* leaves are on average quite a bit greater than *P. triste* leaves. We speculate that larger, heavier leaves may be less able to move if movement is controlled by passive responses to physical changes such as differential turgor across the petiole, blade and rachis. Nevertheless, even if controlled by passive processes allowed by the anatomy of leaf, the increase in cosine i in each species demonstrates that these movements are consistent with patterns of movement that indicate solar tracking, a leaf behavior that has been experimentally shown to increase fitness (Mooney & Ehleringer 1978; Forseth & Ehleringer 1983; Santos *et al.* 2006).

Despite differences in shape and movement, *P. triste* and *P. lobatum* leaves remained close to ambient temperatures over the course of the day, a pattern also found across a wide survey of leaf temperatures measured in the field (Hegazy & El Amry 1998). Interestingly, the maximum daily temperature for both species hovered around 21 degrees, a temperature that Helliker and Richter (2008) proposed leads to maximal rates of photosynthesis due to optimization of CO_2 assimilation. During the winter growing season in South Africa, when air temperatures are cool and plants are not water stressed, without solar tracking and the resulting increased amount of solar radiation on the leaf surface, *P. triste* was predicted to be cooler than ambient, so that solar tracking raised leaf temperatures to near optimum for maximum photosynthetic rates.

Leaf temperatures measured in the field diverged from predictions based on leaf energy budgets. *Pelargonium lobatum* leaves were up to 7 degrees cooler than predicted by leaf energy budget equations based on leaf angle, stomatal conductance, windspeed, air temperature and solar position, even when aspects of leaf shape were more accurately estimated than is generally done. We suspect that the difference between actual leaf temperatures and predictions can be explained by our violations of the assumptions of the leaf energy budget equations. These equations assume that leaves are planar and evenly illuminated across their surface, neither of which are true for our study system, or for most leaves. Both leaf flatness and evenness of light absorption are affected by leaf shape.

In *P. triste*, high levels of lamina dissection result in numerous freely projecting leaflets that are oriented skyward at a variety of angles. Consequently, *P.*

triste leaflets intercept more light than predicted when the sun is low in the sky based on cosine i (predictions are based on a flat, two-dimensional leaf surface), thus facilitating the rapid warming of these leaves early in the day. Under midday conditions when whole-leaf orientation is most normal to the sun, as indicated by the angle of inclination of the rachis, only then outwardly- projecting tips of the leaflets are exposed to direct light. Leaflets scatter incident light such that the majority of the leaflets are experiencing diffuse light, a phenomena that has also been demonstrated in stilt palms (Rich, Holbrook & Luttinger 1995).

An additional consequence of the three-dimensional arrangement of leaflets in *P. triste* is that actual leaf temperatures are nearly 3°C cooler at midday than expected based on energy budgets. This allows leaves to avoid overheating in the middle of the day and to maximize diffuse light interception when there is the risk of photoinhibition. Despite the larger effect of direct light on leaf temperatures, diffuse light is highly effective for photosynthesis (Alton *et al.* 2007) and a more vertical leaf angle reduces irradiance but increases reflectance. Palisade parenchyma is important in receiving light energy for photosynthesis, and the occurrence of this cell layer has been associated with the direction and quality of light across a range of species (Vogelmann & Martin 1993). Our proposition that leaf dissection in *P. triste* increases diffuse light absorption is further supported by the isolateral distribution of palisade mesophyll cells in this species, which has been shown to be correlated with three-dimensional leaf shape and the primary source of light (direct or diffuse) in other studies (Ustin, Jacquemoud & Govaerts 2001; Habermann *et al.* 2011; Joesting, Sprague & Smith 2012).

Leaf shape in *P. lobatum* has a different effect on leaf temperatures because of its more planar shape. Based on energy budgets, leaves of *P. lobatum* were predicted to be several degrees above ambient but observed leaf temperatures tracked ambient very closely. We attribute this difference to large areas of shade on the leaves caused by self-shading of the curled margins of the large lobes, particularly when the sun is low in the sky. Consequently, *P. lobatum* lags in morning warming relative to *P. triste* and to ambient temperatures. In contrast to *P. triste*, at midday, *P. lobatum* has proportionately more leaf surface area exposed to direct light but also more leaf area in total shade, due to lobing and curling at the leaf margins. Consistent with a strong reliance on direct incident light, *P. lobatum* has a bilateral distribution of palisade cells.

To examine the consequences of leaf shape on light interception for daily carbon gain, we computed estimates of integrated carbon gain for one leaf over one day for *P. triste* and *P. lobatum* by multiplying the leaf area exposed to direct light by rates of photosynthesis measured on these populations the same time of year. A_{max} values (18.3 μmol CO^2 m^{-2} s^{-1} for *P. triste* and 19.7 μmol CO^2 m^{-2} s^{-1} for *P. lobatum*) were not significantly different. Because there are significant differences in the leaf area exposed to direct light during the day, estimates of leaf-level integrated carbon gain for one day were three times higher per leaf for *P. lobatum* than for *P. triste* (Fig. 12) (1035 μmol versus 297 μmol carbon, respectively). Even if we include direct plus diffuse light multiplied by the proportion of leaf area experiencing these light regimes, the total difference in integrated carbon gain for *P. lobatum* and *P.*

triste remains similar as both species have similar proportions of diffuse light on their laminas throughout the day.

It is tempting to extrapolate these differences in leaf level carbon gain across the growing season and to conclude that individual *P. triste* leaves are comparatively less productive, but additional advantages of the dissected leaf shape may play out most dramatically as summer approaches. Average daytime temperatures leading into summer dormancy at De Hoop vary from 19°C in September to 23°C in November (Schulze 2007) and rise to as high as 36°C in some parts of the range of *P. lobatum*. All else being equal, midday leaf temperatures of directly illuminated regions of the leaf would be predicted to reach 40°C under spring-time growing conditions at De Hoop. Nicotra and colleagues (2008) showed that photosynthetic thermal optimum for 6 species of *Pelargonium* is around 30°C but that photosynthetic rates declined once temperatures exceeded 33°C. The combined effects of summer temperatures and maximum light interception from a sun that is higher in the sky are likely to lead to damaging leaf temperatures in *P. lobatum*. In *P. triste*, on the other hand, if leaflet orientation remains projected and absorption of direct light in the middle of the day is minimized, predicted leaf temperatures would reach 26° as summer approaches at De Hoop, allowing the leaf to maintain temperatures favorable for photosynthesis well into the summer. These predictions are supported by differences in predicted leaf survivorship quantified in these populations of *P. triste* and *P. lobatum* in 2012: *P. triste* leaves are likely to live 26 days longer. In addition, leaves of *P. triste* also are less likely to experience photoinhibition. Hence, we propose the combination of leaf shape and solar tracking

may be directly linked to differences in leaf longevity in these exposed geophytes through their modulation of direct light absorption and the downstream effects on leaf thermodynamics and photosynthetic rate.

We propose that the effects on leaf shape that may allow *P. triste* leaves to live longer at a given site may also explain differences in distributions of the two species (Fig. 13) (Martinez-Cabrera 2010). Effects of leaf shape that allow *P. triste* to remain cool enough for long-term photosynthetic function at De Hoop may also explain why *P. triste* extends into regions of the more arid Northern Cape of South Africa relative to *P. lobatum*. The latter's more restricted distribution in the CFR, where conditions are more mesic and early summer temperatures are not as warm, is consistent with a leaf with a larger, flatter surface that optimizes photosynthesis during the winter growing season.

Conclusion

While variation in leaf size has been linked to climate at broad scales, the significance of variation in leaf size and leaf shape at smaller, local scales is not well understood. Even within a single site, species vary tremendously in leaf size and shape, to the extent that across global data sets, leaf size and shape are only weakly correlated with climate (Reich & Cornelissen 2014) and these authors conclude that neither are functional leaf traits. In contrast, we suggest that species differences in leaf shape and solar tracking behavior may promote the co-occurrence of *P. triste* and *P. lobatum* via different strategies (see also the classic study by Mooney and Ehleringer, 1978). Leaf movements in *P. triste* and *P. lobatum* adjust the amount and quality of light intercepting the lamina, and so leaf orientation and the thermal properties of leaf shape affect leaf temperature and ultimately appear to greatly affect daily carbon gain. Variation in SLA between these species is relatively minor compared to the dramatic effects of leaf shape and anatomy on light absorption. If leaf shape and movement potentially lower summertime leaf temperatures and are associated with greater leaf longevity, then these traits not only indicate different functional strategies of co-existence in these closely related species but also go a long way in explaining differences in their distributions, perhaps offering greater "service to the plant" than even Darwin anticipated.

References

Adobe Photoshop CS4 Extended (2008) Adobe Systems Incorporated.

Alton, P.B., Ellis, R., Los, S.O. & North, P.R. (2007) Improved global simulations of gross primary product based on a separate and explicit treatment of diffuse and direct sunlight. *Journal of Geophysical Research-Atmospheres,* **112**.

Balding, F.R. & Cunningham, G.L. (1976) A comparison of heat transfer characteristics of simple and pinnate leaf models. *Botanical Gazette,* **137,** 65-74.

Colchero, F., Jones, O.R. & Rebke, M. (2012) BaSTA: an R package for Bayesian estimation of age-specific survival from incomplete mark-recapture/recovery data with covariates. *Methods in Ecology and Evolution,* **3,** 466-470.

Cornwall, C., Horiuchi, A. & Lehman, C. (2014) Solar position calculator. National Oceanic and Atmospheric Administration Surface Radiation Research Branch. Retreived from: http://www.srrb.noaa.gov/highlights/sunrise/azel.html Accessed June 8, 2009.

Cowling, R., Richardson, D. & Pierce, S. (1997) Vegetation of Southern Africa. Cambridge University Press, New York.

Darwin, C. (1881) *The Power of Movement in Plants*. Appleton, New York.

Ehleringer, J.R. & Forseth, I.N. (1980) Solar Tracking by Plants. *Science,* **210,** 1094-1098.

Esler, K.J., Rundel, P.W. & Vorster, P. (1999) Biogeography of prostrate-leaved geophytes in semi-arid South Africa: hypotheses on functionality. *Plant Ecology,* **142,** 105-120.

Forseth, I.N. & Ehleringer, J.R. (1983) Ecophysiology of two solar tracking desert winter annuals III. Gas exchange responses to light, CO2 and VPD in relation to long-term drought. *Oecologia,* **57,** 344-351.

Forseth, I.N. & Teramura, A.H. (1986) Kudzu leaf energy budget and calculated transpiration: the influence of leaflet orientation. *Ecology,* **67,** 564-571.

Fujita, K., Takagi, S. & Terashima, I. (2008) Leaf angle in Chenopodium album is determined by two processes: induction and cessation of petiole curvature. *Plant Cell and Environment,* **31,** 1138-1146.

Fukuda, N., Fujita, M., Ohta, Y., Sase, S., Nishimura, S. & Ezura, H. (2008) Directional blue light irradiation triggers epidermal cell elongation of abaxial side resulting in inhibition of leaf epinasty in geranium under red light condition. *Scientia Horticulturae,* **115,** 176-182.

Galvez, D. & Pearcy, R.W. (2003) Petiole twisting in the crowns of Psychotria limonensis: implications for light interception and daily carbon gain. *Oecologia,* **135,** 22-29.

Gates, D.M., Alderfer, R. & Taylor, E. (1968) Leaf Temperatures of Desert Plants. *Science,* **159,** 994-995.

Geller, G. & Smith, W. (1982) Influence of Leaf Size, Orientation, and Arrangement on Temperature and Transpiration in Three High-Elevation, Large-Leafed Herbs. *Oecologia,* **53,** 227-234.

Goldblatt, P. & Manning, J.C. (2002) Plant Diversity of the Cape Region of Southern Africa. *Annals of the Missouri Botanical Garden,* **89,** 281-302.

Grace, J., Fasehun, F. & Dixon, M. (1980) Boundary layer conductance of the leaves of some tropical timber trees. *Plant Cell and Environment,* **3,** 443-450.

Habermann, G., Ellsworth, P.F.V., Cazoto, J.L., Feistler, A.M., da Silva, L., Donatti, D.A. & Machado, S.R. (2011) Leaf paraheliotropism in Styrax camporum confers increased light use efficiency and advantageous photosynthetic responses rather than photoprotection. *Environmental and Experimental Botany,* **71,** 10-17.

Hegazy, A. & El Amry, M. (1998) Leaf temperature of desert sand dune plants: perspectives on the adaptability of leaf morphology. *African Journal of Ecology,* **36,** 34-43.

Hernandez, L.F. (2010) Leaf angle and light interception in sunflower (Helianthus annuus L.). Role of the petiole's mechanical and anatomical properties. *Phyton-International Journal of Experimental Botany,* **79,** 109-115.

Joesting, H.M., Sprague, M.O. & Smith, W.K. (2012) Seasonal and diurnal leaf orientation, bifacial sunlight incidence, and leaf structure in the sand dune herb Hydrocotyle bonariensis. *Environmental and Experimental Botany,* **75,** 195-203.

Jones, C.S., Bakker, F.T., Schlichting, C.D. & Nicotra, A.B. (2009) Leaf shape evolution in the South African genus Pelargonium L'Her. (Geraniaceae). *Evolution; international journal of organic evolution,* **63,** 479-497.

Jones, C.S., Martinez-Cabrera, H.I., Nicotra, A.B., Mocko, K., Marais, E.M. & Schlichting, C.D. (2013) Phylogenetic influences on leaf trait integration in Pelargonium (Geraniaceae): convergence, divergence, and historical adaptation to a rapidly changing climate. *American Journal of Botany,* **100,** 1306-1321.

Martinez-Cabrera, H.I. (2010) Influence of climate in functional and species diversification in South African Pelargonium. PhD, University of Connecticut.

Mooney, H.A. & Ehleringer, J.R. (1978) The carbon gain benefits of solar tracking in a desert annual. *Plant, Cell and Environment,* **1,** 307-311.

Niinemets, U. (1998) Adjustment of foliage structure and function to a canopy light gradient in two co-existing deciduous trees. Variability in leaf inclination angles in relation to petiole morphology. *Trees-Structure and Function,* **12,** 446-451.

Nobel, P.S. (1983) *Biophysical Plant Physiology and Ecology*. W.H. Freeman, San Francisco.

Parkhurst, D. & Loucks, O. (1972) Optimal Leaf Size in Relation to Environment. *Ecology,* **60,** 505-537.

Pearman, G., Weaver, H. & Tanner, C. (1972) Boundary Layer Heat Transfer Coefficients Under Field Conditions. *Agricultural Meteorology,* **10,** 83-92.

Prichard, J.M. & Forseth, I.N. (1988) Rapid Leaf Movement, Microclimate, and Water Relations of Two Temperate Legumes in Three Contrasting Habitats. *American Journal of Botany,* **75,** 1201-1211.

R Development Core Team (2012) R: A Language and Environment for Statistical Computing. R Foundation for Statistical Computing Vienna, Austria, Retrieved from: http://www.R-project.org/ Accessed Oct 26, 2012

Reich, P.B. & Cornelissen, H. (2014) The world-wide 'fast-slow' plant economics spectrum: a traits manifesto. *Journal of Ecology,* **102,** 275-301.

Rich, P., Holbrook, N. & Luttinger, N. (1995) Leaf Development and Crown Geometry of Two Iriareoid Palms. *American Journal of Botany,* **82,** 328-336.

Rosa, L.M. & Forseth, I.N. (1996) Diurnal patterns of soybean leaf inclination angles and azimuthal orientation under different levels of ultraviolet-B radiation. *Agricultural and Forest Meteorology,* **78,** 107-119.

Rossa, B. & von Willert, D.J. (1999) Physiological characteristics of geophytes in semi-arid Namaqualand, South Africa. *Plant Ecology,* **142,** 121-132.

Santos, A., Rosa, L., Franke, L. & Nabinger, C. (2006) Heliotropism and water availability effects on flowering dynamics and seed production in Macroptilium lathyroides. *Revista Brasileira de Sementes,* **28,** 45-52.

Schuepp, P. (1993) Tansley Review No. 59 Leaf boundary layers. *New Phytologist,* **125,** 447-507.

Schulze, R. (2007) The South African atlas of agrohydrology and climatology, Technical Report WRC Report 1489/1/06. Water Research Commission, Pretoria, South Africa.

Sousa, W. (2003) Tleaf2.xls: Leaf energy balance simulation program. *Laboratory exercise for plant ecophysiology* (ed. T. Dawson). University of California,

Berkeley, CA. Retreived from: http://ib.berkeley.edu/courses/ib151/Tleaf2.xls Accessed June 10, 2014.

Ustin, S.L., Jacquemoud, S. & Govaerts, Y. (2001) Simulation of photon transport in a three-dimensional leaf: implications for photosynthesis. *Plant Cell and Environment,* **24,** 1095-1103.

van Zanten, M., Pons, T.L., Janssen, J.A.M., Voesenek, L. & Peeters, A.J.M. (2010) On the Relevance and Control of Leaf Angle. *Critical Reviews in Plant Sciences,* **29,** 300-316.

Vogelmann, T. & Martin, G. (1993) The functional significance of palisade tissue: penetration of directional versus diffuse light. *Plant, Cell and Environment,* **16,** 65-72.

Table 1. Summary of mean leaf traits for *P. triste* and *P. lobatum* leaves. Values represent the mean of five leaves ± one standard error. F and P values of ANOVAs, level of significance indicated as *** P<0.001, ** P<0.01 and * P<0.05.

	P. triste	*P. lobatum*	F value	P value
Lamina length (cm)	10.3 ± 1.5	9.4 ± 0.9	0.232	0.643
Lamina width (cm)	8.8 ± 0.8	10.4 ± 0.9	1.781	0.219
Lamina area (cm^2)	20.5 ± 1.4	48.1 ± 3.4	55.69	1.44e-09***
Specific Leaf Area (SLA) (cm^2/g)	87.4 ± 2.9	113.1 ± 2.5	46.02	1.58e-08***
Leaf Dissection Index (LDI)	31.4 ± 1.7	7.2 ± 0.3	200	3.43e-11***
D (flat – projected leaf area) (cm^2)	4.5 ± 0.5	4.3 ± 0.4	0.097	0.758
Functional leaf size (FLS) (cm)	0.10 ± 0.00	3.90 ± 0.26	169.9	1.14e-06***
Abaxial Stomatal conductance (mmol H_2O $m^{-2}s^{-1}$)	205 ± 68	98 ± 16	2.33	0.18
Adaxial Stomatal conductance (mmol H_2O $m^{-2}s^{-1}$)	184 ± 25 a	147 ± 41	0.62	0.46
Total Stomatal conductance (mmol H_2O $m^{-2}s^{-1}$)	389 ± 89	245 ± 56	1.89	0.22

(a)

(b)

Figure 1. *P. triste* (a) and *P. lobatum* (b); photographs show one representative leaf at 13:00.

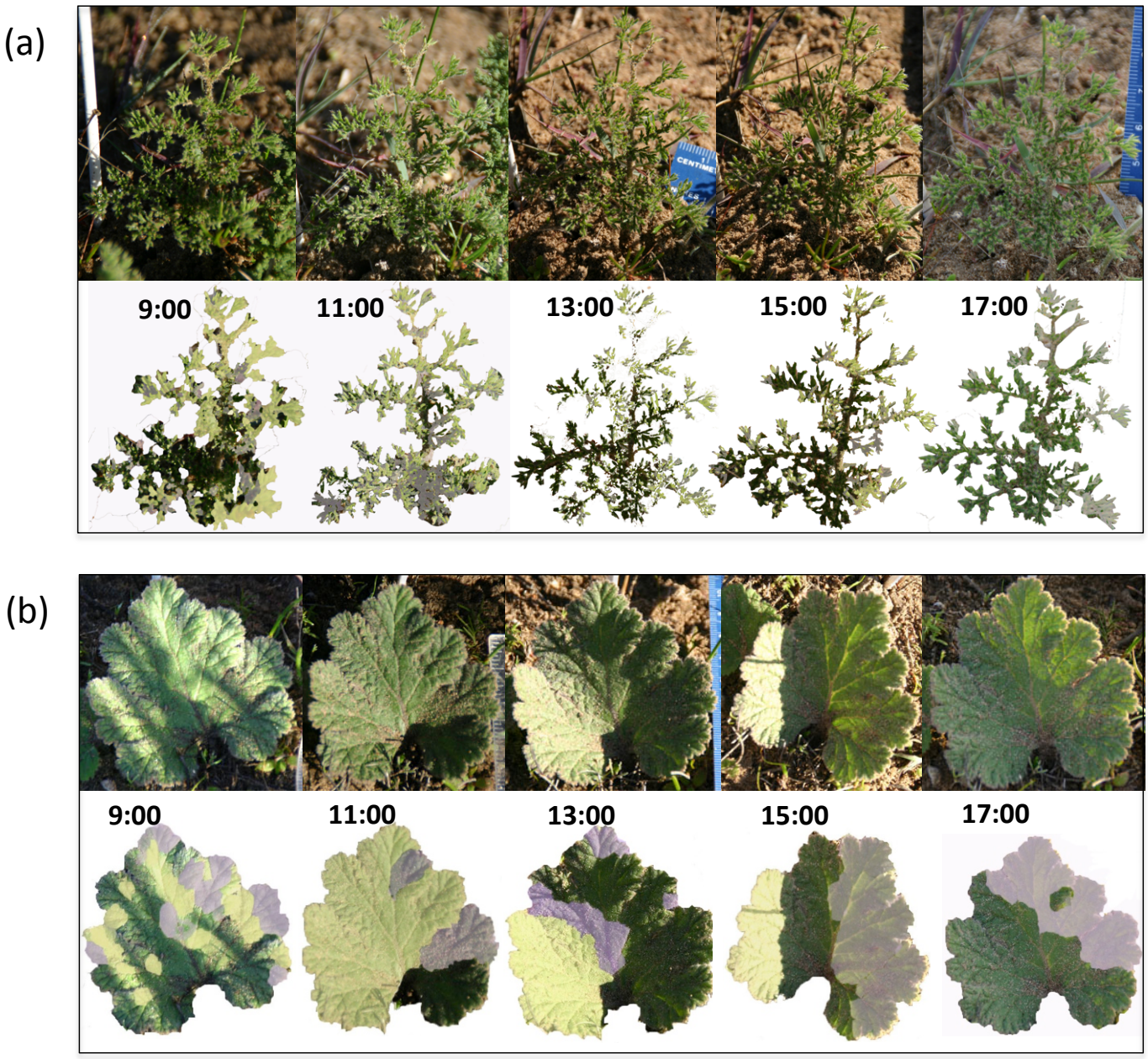

Figure 2. One representative *P. triste* leaf (a) and *P. lobatum* leaf (b) across the diurnal time course. On analyzed images, yellow indicates direct light interception, purple is diffuse light and green regions are in shade.

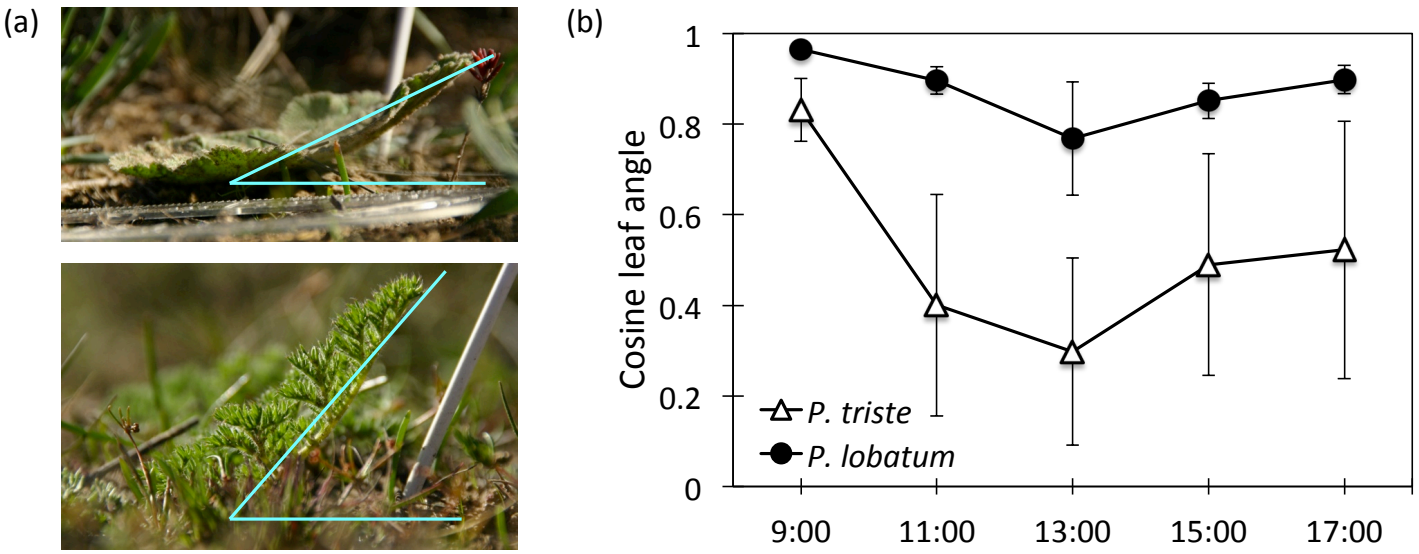

Figure 3. (a) Leaf inclination at 13:00 for *P. lobatum* (upper) and *P. triste* (lower). (b) *P. triste* (open triangles) moves more during the day than *P. lobatum* (solid circles). Cosine leaf angle represents changes in leaf inclination and azimuth; in a stationary leaf, cosine leaf angle = 1. Symbols represent mean of 5 leaves of each species and error bars are ± one standard error.

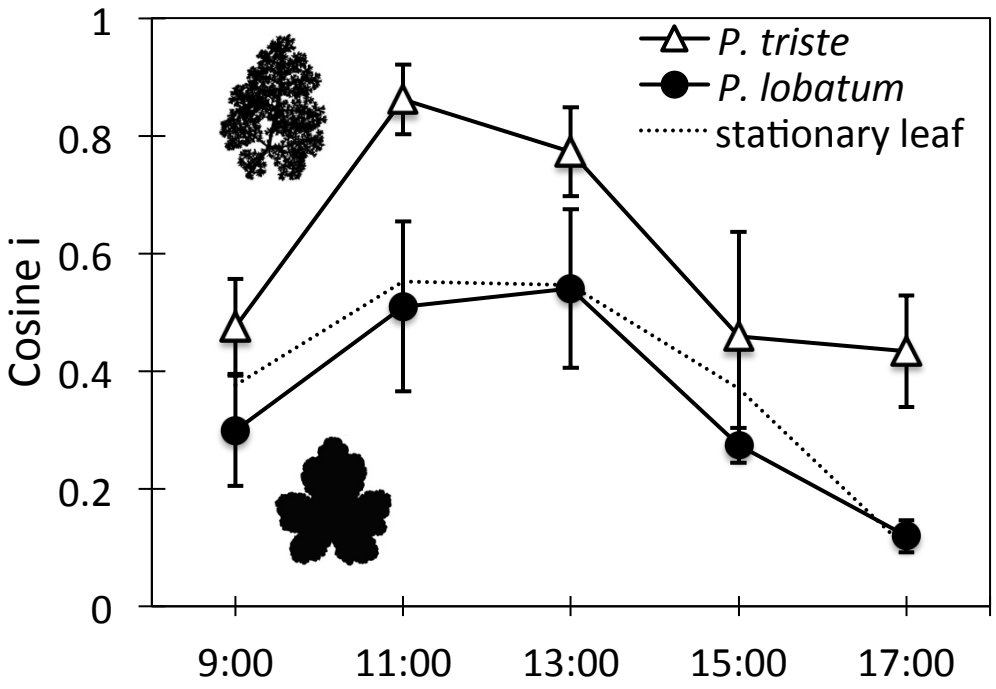

Figure 4. *P. triste* leaves (open triangles) are oriented more directly to the sun than *P. lobatum* leaves (solid circles). Symbols represent mean of 5 leaves of each species and error bars are ± one standard error. The dotted line represents incident light interception for a stationary leaf.

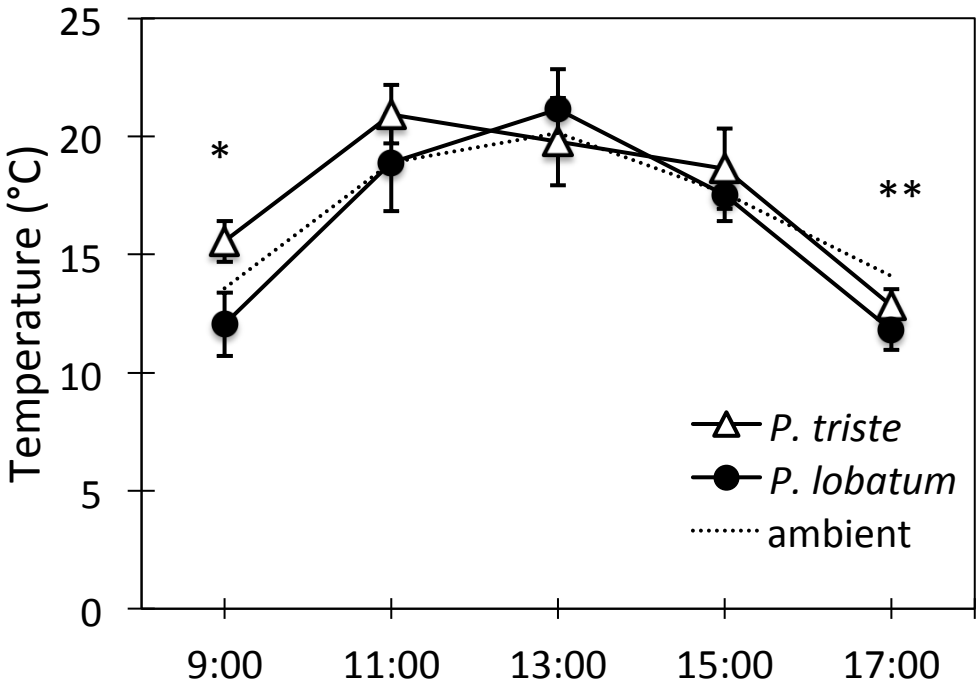

Figure 5. Leaf temperatures for *P. triste* (open triangles) and *P. lobatum* (solid circles) across the diurnal time course. Symbols represent mean of 5 leaves of each species and error bars are ± one standard error. The dotted line represents ambient air temperatures. *P. triste* and *P. lobatum* leaf temperatures are significantly different at 9:00, and *P. lobatum* leaves are significantly cooler than ambient at 17:00. Asterisks indicate P-value significance of TukeyHSD test, ** $P<0.01$ and * $P<0.05$.

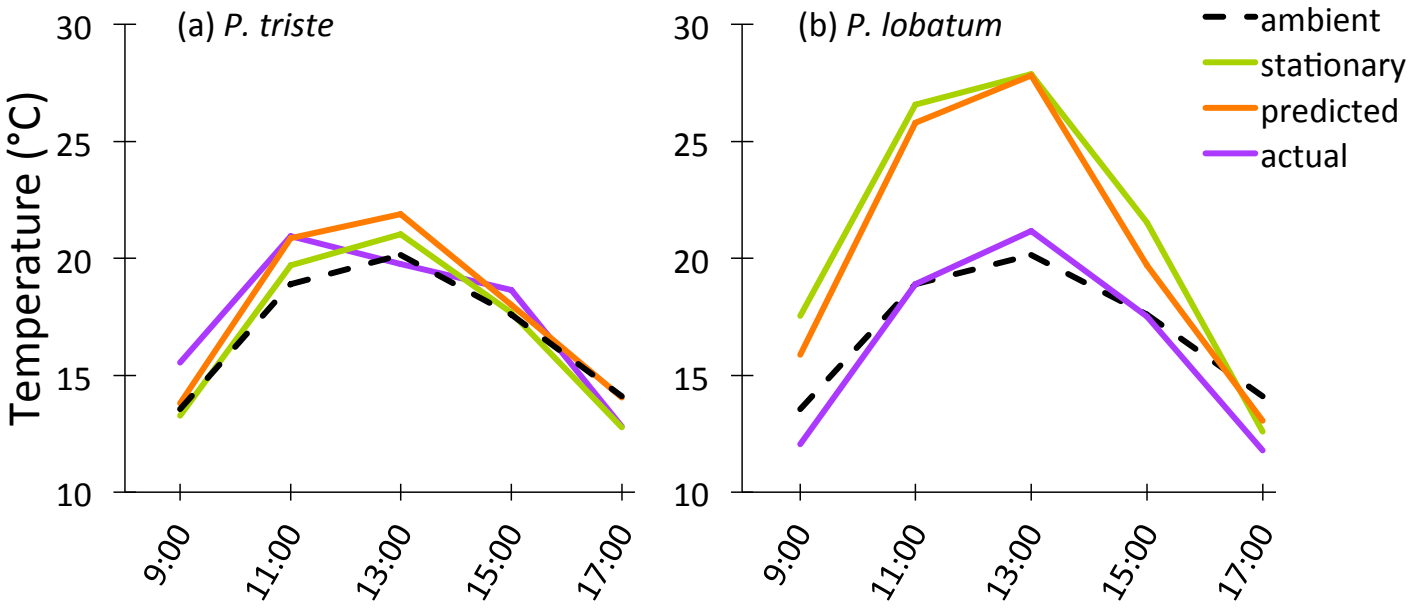

Figure 6. Leaf temperatures for *P. triste* (a) and *P. lobatum* (b). Leaf energy budgets were used to calculate leaf temperatures for stationary leaves (green line) and predicted leaf temperatures based on observed orientation of the leaves (orange line). We compare these calculations to actual leaf temperatures measured in the field (purple line) and ambient air temperature (dashed line).

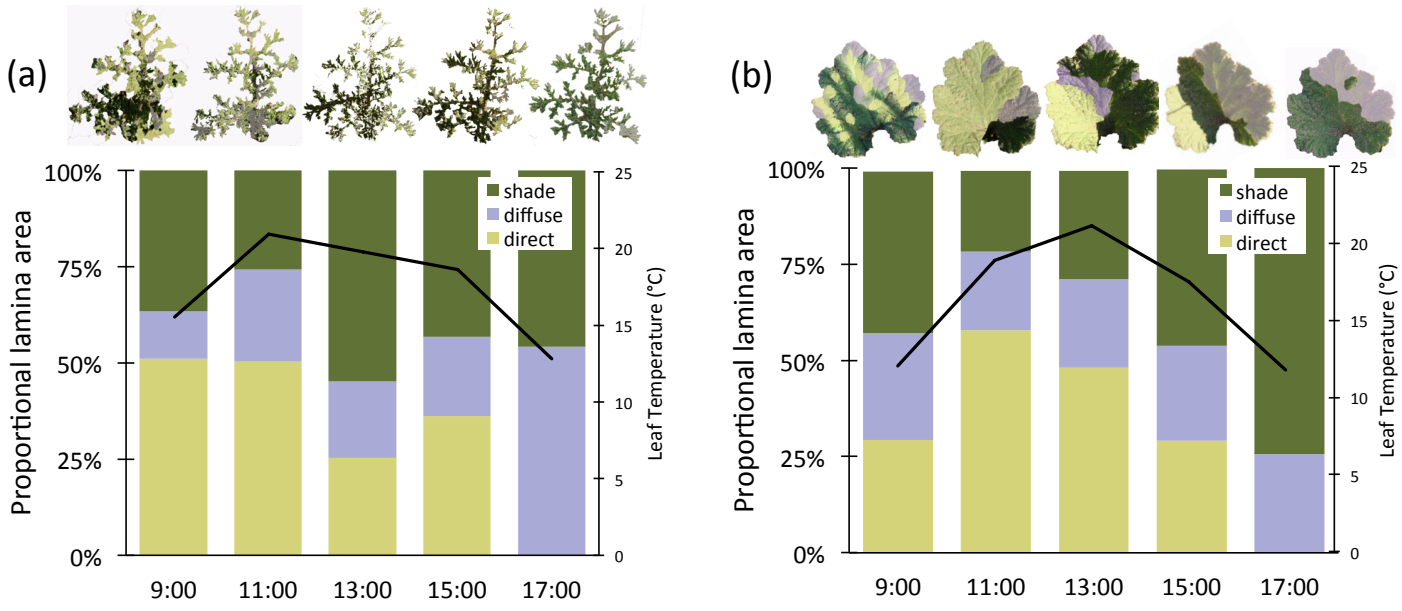

Figure 7. The proportion of *P. triste* (a) and *P. lobatum* (b) laminas exposed to direct light (yellow bars), diffuse light (purple bars) and shaded (green bars); bars represent the mean values of five leaves across the diurnal time course. Leaf images shown represent one individual across time. Measured leaf temperatures (black line) are plotted over the bars.

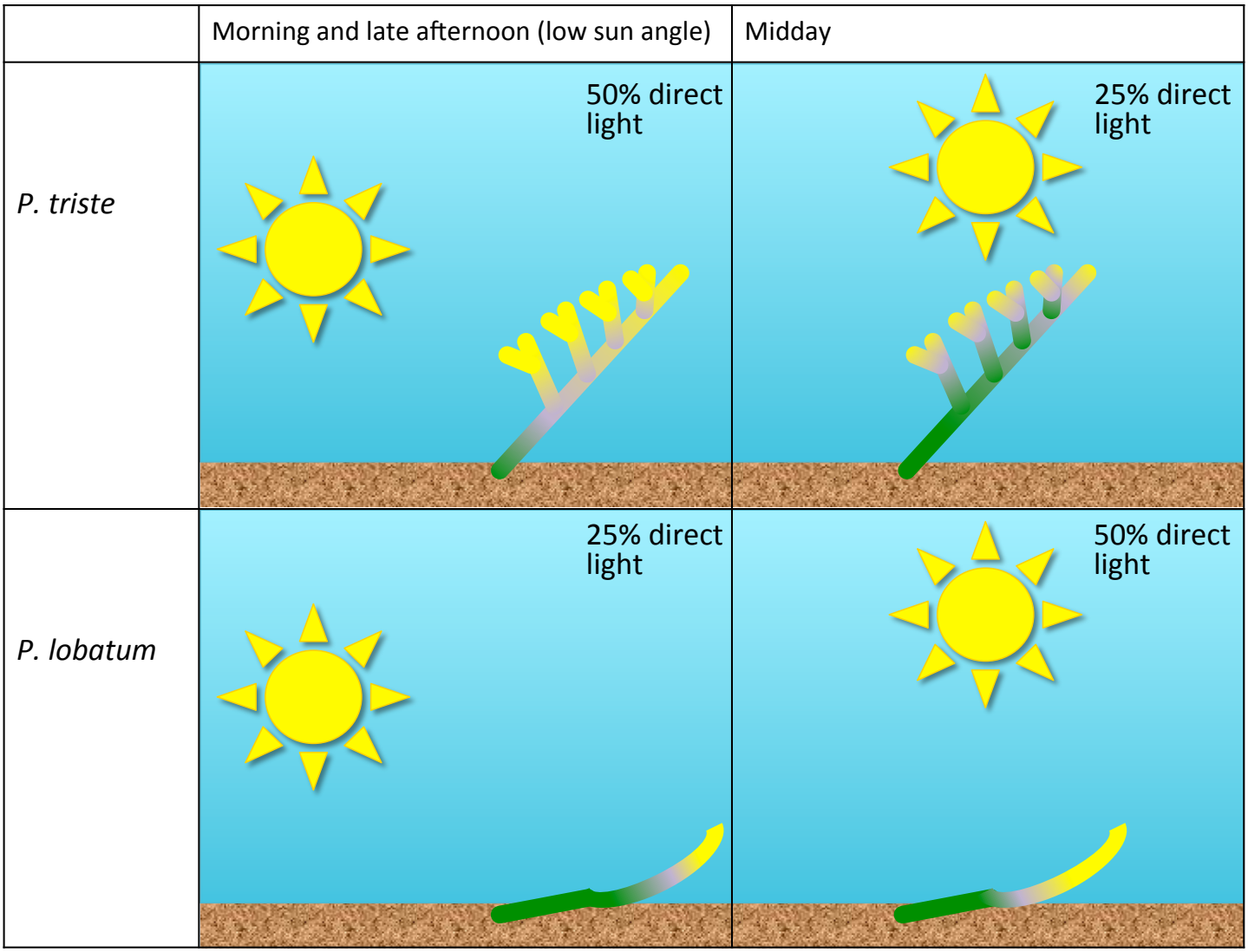

Figure 8. Schematic diagram for *P. triste* and *P. lobatum* shows how leaf architecture and solar angle influence light interception. Direct light (yellow regions on leaf cartoons) is maximized in the morning and late afternoon in *P. triste*, while *P. lobatum* experiences more diffuse light (purple) and shade (green) at low sun angles.

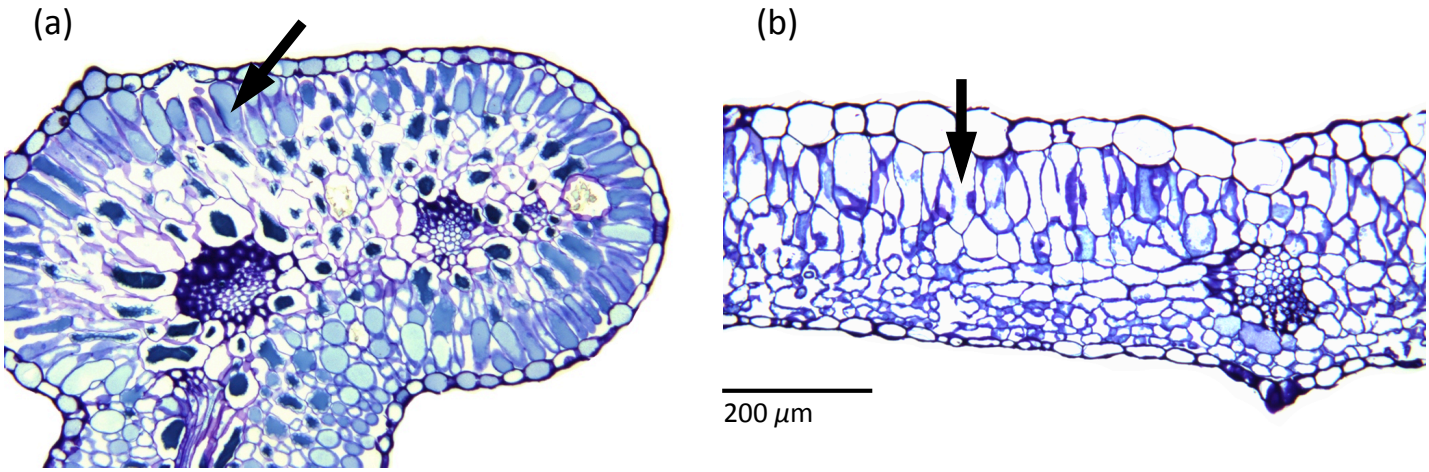

Figure 9. Leaf cross sections of *P. triste* (a) and *P. lobatum* (b) show differences in leaf transectional symmetry and the distribution of palisade parenchyma cells (arrows). Scale bar applies to both images.

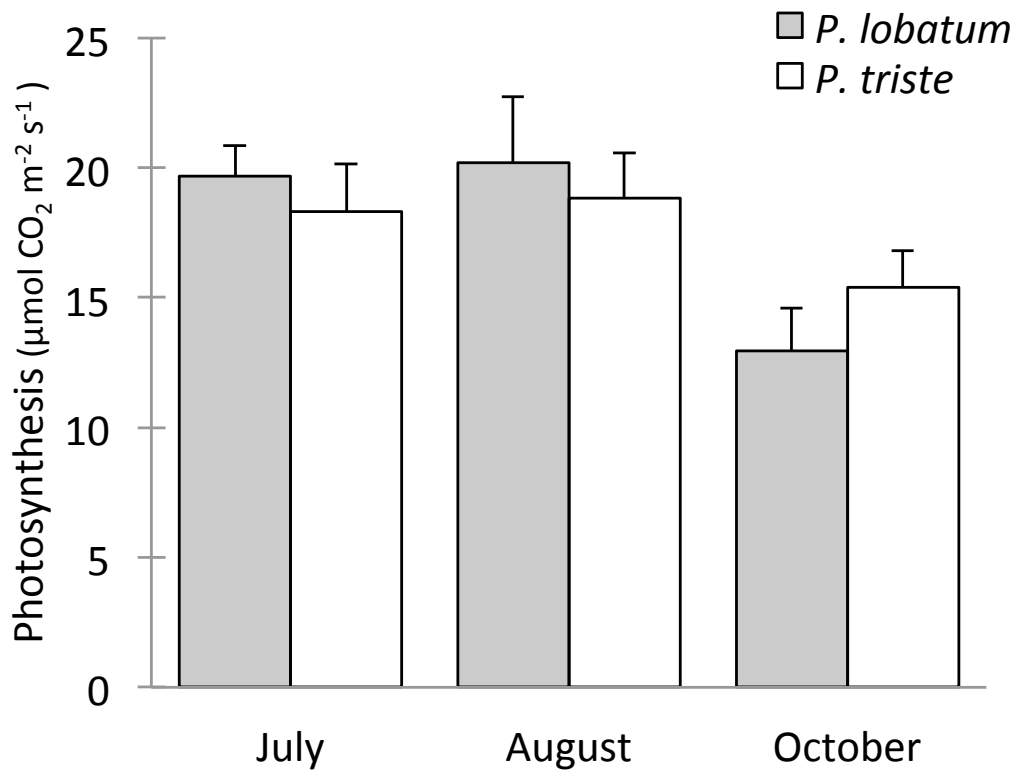

Figure 10. Mean photosynthetic rates for De Hoop populations of *P. lobatum* and *P. triste* during the 2012 growing season. Bars represent the mean value of 4-8 plants per species and error bars indicate +1 standard error.

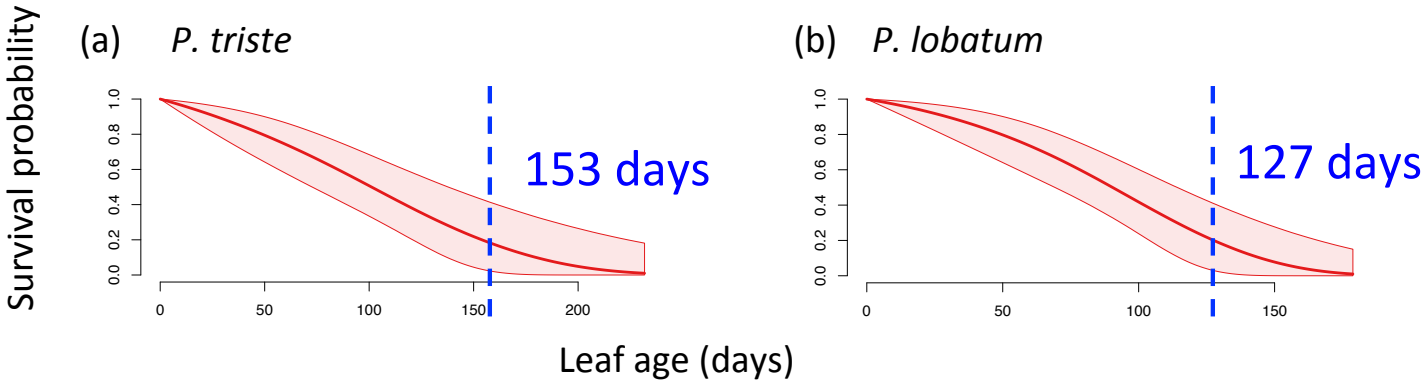

Figure 11. Survivorship curves show differences in predicted leaf lifespans for *P. triste* (a) and *P. lobatum* (b); graphs represent population values computed from 2012 census data. Blue line indicates estimated leaf lifespan for a single leaf, or leaf age where survival probability equals zero.

Figure 12. Integrated carbon gain for one *P. lobatum* leaf (solid line) and one *P. triste* leaf (dashed line) under winter growing conditions; calculations are based on A_{max} and total leaf area exposed to direct light.

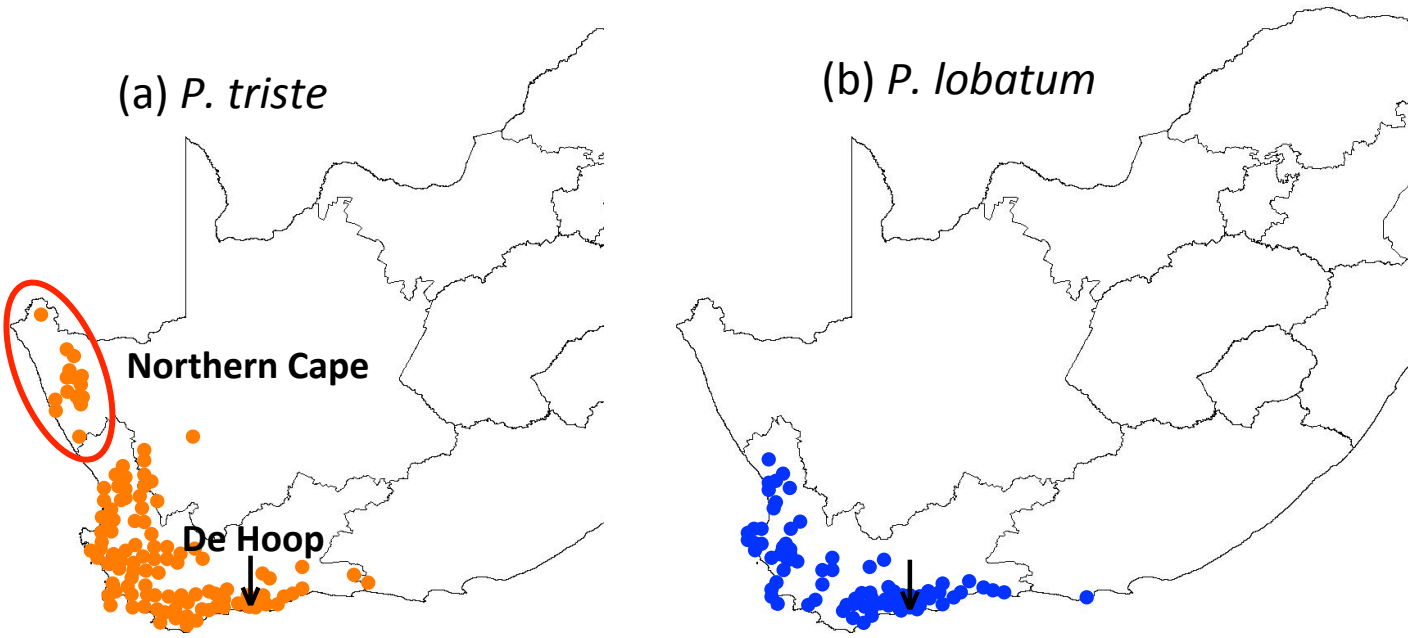

Figure 13. Distribution maps of *P. triste* (a) and *P. lobatum* (b), points indicate species occurrences based on climatic data (Martinez-Cabrera 2010). *Pelargonium triste* extends into more arid regions of the Northern Cape (red oval).

Appendix Table 1. Leaf energy balance equation used to predict leaf temperatures (Sousa 2003):

$$T_l = T_a + ((\text{Total Energy In} / 2 - (\varepsilon * \sigma * ((T_a + 273.15)^4)) - ((L * (23 - e_a)) / (r_l + (K_l * ((w / v) \wedge 0.5) / D_j)))) / (4 * \varepsilon * \sigma * ((T_a + 273.15)^3) + h_c + ((L * \Delta) / (r_l + (K_l * ((w / v) \wedge 0.5) / D_j)))))$$

T_l	Leaf temperature
T_a	Air temperature
ε	Absorption coefficient to solar radiation
σ	Stephan Boltzman constant (blackbody radiation constant)
L	Latent heat of vaporization
e_a	Water vapor density of air
r_l	Leaf resistance to water vapor
K_l	Leaf shape parameter
w	Leaf length in the direction of the wind
v	Wind velocity
D_j	Diffusion coefficient for water vapor
h_c	Convection coefficient
Δ	Slope of vapor pressure-T curve

Appendix Table 2. Mean leaf temperatures of five leaves of *P. triste* (a) and *P. lobatum* (b) measured across the diurnal time course (Observed T), energy budget predictions for inclined leaves (Predicted T), energy budget predictions for stationary leaves (leaves that do not incline during the day) (Stationary T) and measured air temperatures (Ambient T). The mean angle of inclination (Inclination), potential incident light interception for inclined leaves (Cosine i) and the mean proportions of the lamina surface actually experiencing direct light, diffuse light and shade.

(a) *P. triste*

Time	9:00	11:00	13:00	15:00	17:00
Observed T (°C)	15.6	20.9	19.8	18.6	12.8
Predicted T (°C)	13.8	20.9	21.9	18.0	14.0
Stationary T (°C)	13.3	19.7	21.0	17.7	12.8
Ambient T (°C)	13.6	18.9	20.2	17.6	14.1
Inclination (°)	31.2	42.0	47.4	42.2	36.8
Cosine i	0.48	0.86	0.77	0.46	0.43
Direct light (%)	51.1	50.3	25.3	36.2	0.0
Diffuse light (%)	12.2	24.0	19.9	20.5	54.1
Shade (%)	36.7	25.7	54.9	43.3	45.9

(b) *P. lobatum*

Time	9:00	11:00	13:00	15:00	17:00
Observed T (°C)	12.0	18.9	21.2	17.5	11.8
Predicted T (°C)	15.9	25.8	27.8	19.7	13.1
Stationary T (°C)	17.5	26.6	27.9	21.5	12.6
Ambient T (°C)	13.6	18.9	20.2	17.6	14.1
Inclination (°)	12.8	19.8	24.4	19.2	11.6
Cosine i	0.30	0.51	0.54	0.27	0.12
Direct light (%)	29.3	57.8	48.1	29.2	0.0
Diffuse light (%)	27.9	20.4	23.0	24.6	25.6
Shade (%)	42.0	21.1	28.0	45.8	74.4

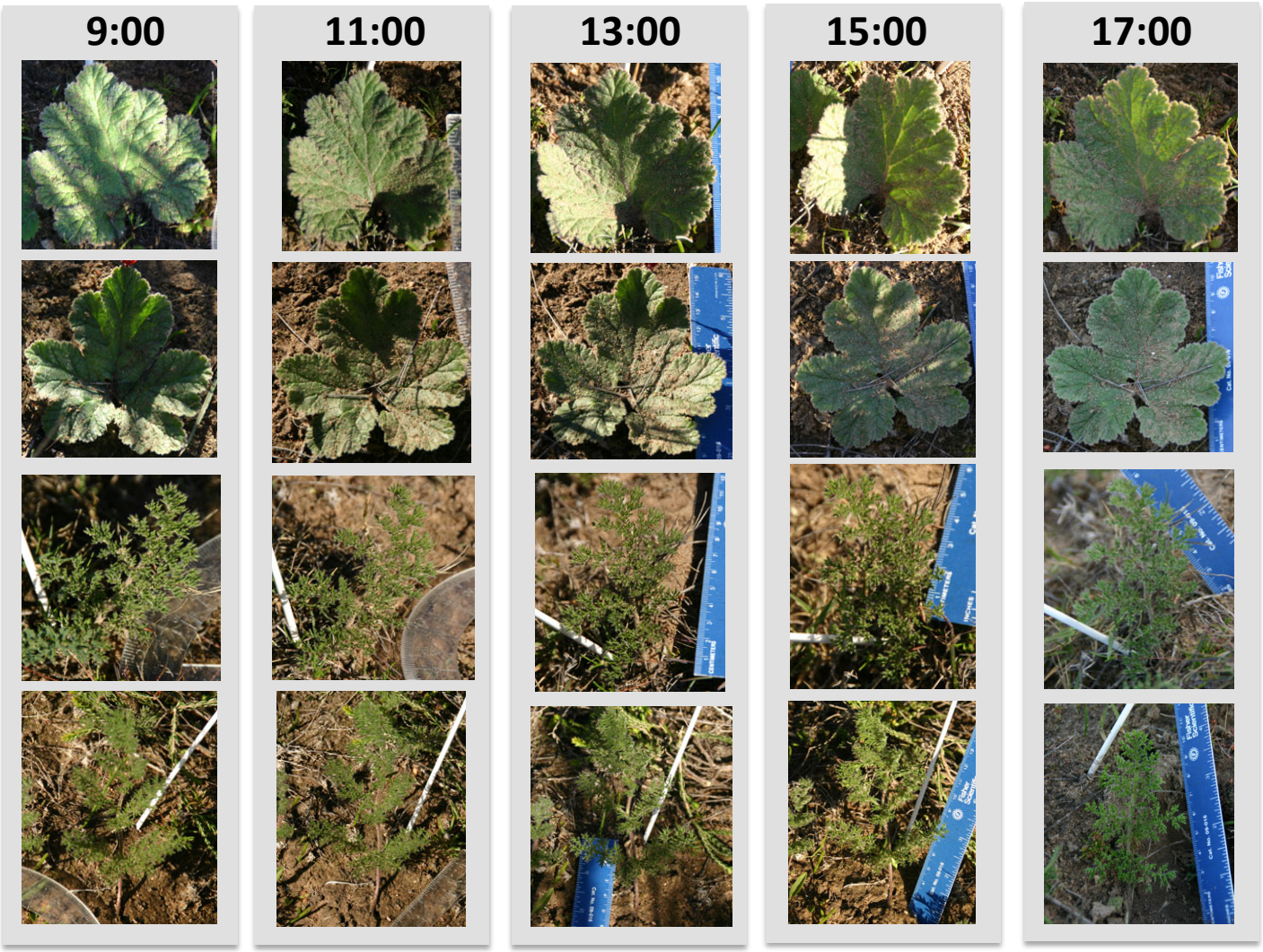

Appendix Figure 1. Face-view photographs of individual *P. lobatum* leaves (upper two rows) and *P. triste* leaves (lower two rows) across the diurnal time course.